

# A kinetically constrained model exhibiting non-linear diffusion and jamming

**Abhishek Raj, Vadim Oganessian**

Physics Program and Initiative for the Theoretical Sciences, The Graduate Center, CUNY, New York, New York 10016, USA  
Department of Physics and Astronomy, College of Staten Island, CUNY, Staten Island, New York 10314, USA

**Antonello Scardicchio**

The Abdus Salam ICTP, Strada Costiera 11, 34151, Trieste (Italy)  
INFN, Sezione di Trieste, Via Valerio 2, 34128, Trieste (Italy).

**Abstract.** We present a classical kinetically constrained model of interacting particles on a triangular ladder, which displays diffusion and jamming and can be treated by means of a classical-quantum mapping. Interpreted as a theory of interacting fermions, the diffusion coefficient is the inverse of the effective mass of the quasiparticles which can be computed using mean-field theory. At a critical density  $\rho = 2/3$ , the model undergoes a dynamical phase transition in which exponentially many configurations become jammed while others remain diffusive. The model can be generalized to two dimensions.

## 1. Introduction

In recent years, we have witnessed a shift of attention in the field of statistical physics from the study of thermodynamic, equilibrium properties, which have been the core of the subject since its inception, to the characterization of the approach to equilibrium, or lack thereof. This is due to theoretical and experimental advances, both in quantum and classical systems. In the first realm, the current degree of control on cold atomic arrays, superconducting qubits arrays, and the availability of new computational resources has spurred a renewed interest in the dynamics of many-body quantum systems and in particular in their approach to equilibrium. The eigenstate thermalization hypothesis [7, 27, 5], and its counterpart for strongly disordered systems, many-body localization (see [2, 17, 1, 16], and the most recent [26]) are two prominent examples of this work. In the classical world, the line of work which started with the equilibrium properties of spin glasses [9, 13] which applies well beyond the original scope [11], and evolved into a theory of complexity [18], is another example. The mean-field theory which comprises replica symmetry breaking, has been successfully applied to computational complexity

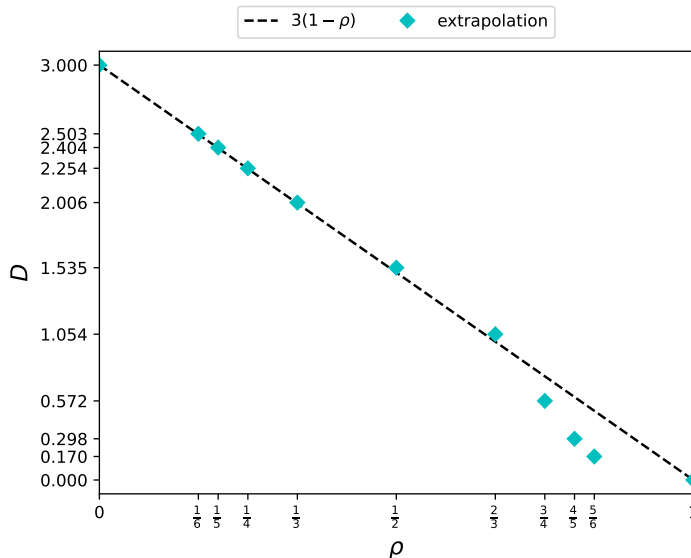


**Figure 1.** Comparison of mean-field solution (dashed straight-line) against extrapolated numerical results (green diamonds) – see Figs. 7 and 8; Notice that the numerical data follow the mean-field prediction of Eq.(26) quite closely until the jamming point  $\rho = 2/3$ . The disagreement at high density may be due to progressively less accurate extrapolation of numerics.

[14, 15], structural glasses [12], and many other examples [19]. In this paper we turn our attention to a classical random process model which has slow dynamics and jamming, and whose solution is obtained by mapping to a model of interacting fermions, thereby connecting the two lines of work.

To achieve this, we consider a model of interacting random walkers with simple constraints, or a *kinetically constrained process* (KCP). KCP's are a widely used tool in statistical mechanics to describe the approach to equilibrium, the emergence of non-equilibrium states, and glassy dynamics [6, 23, 4]. Among other aspects, they are useful to study the emergence, in a controlled setting, of the hydrodynamic behavior and the statistics of large deviations from equilibrium. In this paper, we introduce and study a simple exclusion process in which particles can hop to their left or right conditioned to the fact that *both* the left and right side is empty. The model is easily defined on a triangular ladder, which will allow, in further work, to define it on a triangular lattice.

Our model admits a classical-to-quantum mapping to a frustration-free[10] spin Hamiltonian whose groundstates may be obtained exactly[10]. To demonstrate the existence of a diffusive behavior in the original model we study the dispersion of elementary excitations of the quantum problem – the diffusion coefficient is proportional to the inverse mass of the quasiparticle. By construction, the diffusion coefficient is expected to decrease monotonically with increasing particle density  $\rho$ . We find the diffusion coefficient with a mean-field treatment of the fermionic Hamiltonian and compare against exact numerical results on finite chains, see Fig. 1. The mean-field solution  $D = 3(1 - \rho)$ , where  $\rho$  is the density of particles, agrees surprisingly well with

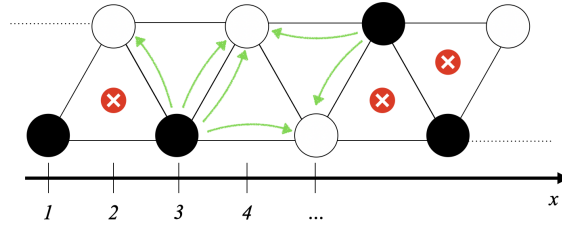


**Figure 2.** The rules for hopping. In active triangles, where only one particle out of 3 is present, it can hop with the same probability along the green arrows. Where two or more particles are present in a triangle (red cross) such triangle is inactive. On the lower axis, the numeration convention we use.

the numerics in a very large range of densities, see Fig.1, which makes us suspect it is an exact solution.

This is more surprising if we consider that the model exhibits the presence of jammed configurations, which appear at a critical density  $\rho = 2/3$ , therefore showing an interesting connection with the study of jamming in granular materials [8, 19, 3].

## 2. The model

The random process studied describes the update of 3 particles configurations where the only mobile configurations are those in which a particle is free on both sides. The rationale behind this choice is to avoid any particle-hole symmetry, in such a way to guarantee a monotonically decreasing diffusion coefficient. The rule is sketched in Figure 2.

In order to write the rate matrix we choose the basis 000, 001, ..., 111, where 0 is an empty site and 1 a particle. On these 3 neighboring lattice sites, the matrix of the transition rates is:

$$h_{i,i+1,i+2} = \begin{pmatrix} 0 & 0 & 0 & 0 & 0 & 0 & 0 & 0 \\ 0 & -1 & \frac{1}{2} & 0 & \frac{1}{2} & 0 & 0 & 0 \\ 0 & \frac{1}{2} & -1 & 0 & \frac{1}{2} & 0 & 0 & 0 \\ 0 & 0 & 0 & 0 & 0 & 0 & 0 & 0 \\ 0 & \frac{1}{2} & \frac{1}{2} & 0 & -1 & 0 & 0 & 0 \\ 0 & 0 & 0 & 0 & 0 & 0 & 0 & 0 \\ 0 & 0 & 0 & 0 & 0 & 0 & 0 & 0 \\ 0 & 0 & 0 & 0 & 0 & 0 & 0 & 0 \end{pmatrix} \quad (1)$$

The total rate matrix is

$$H = \sum_{i=1}^L h_{i,i+1,i+2} \quad (2)$$

where we use periodic boundary conditions, and it is a positive matrix, whose ground state energy is  $E_0 = 0$ .  $H$  rules the evolution of probabilities of particle configurations

$$\sigma = \{\sigma_1, \dots, \sigma_L\} \in \{0, 1\}^L$$

$$\dot{P}(\sigma, t) = - \sum_{\sigma, \sigma'} H_{\sigma, \sigma'} P(\sigma', t). \quad (3)$$

The evolution conserves both particle number and momentum so we can select the appropriate  $N, Q$  sector. Time-dependent expectation values of observables  $O$  can be computed as

$$\begin{aligned} \langle O(t) \rangle &= \sum_{\sigma} O(\sigma) P(\sigma, t) = \sum_{\sigma, \sigma'} O(\sigma) (e^{-Ht})_{\sigma, \sigma'} P(\sigma', 0), \\ &= \sum_a e^{-E_a t} \sum_{\sigma, \sigma'} O(\sigma) \langle \sigma | E_a \rangle \langle E_a | P(0) \rangle, \end{aligned} \quad (4)$$

where  $|E_a\rangle$  are the eigenvectors of  $H$ . Any state  $|P(t)\rangle$  has the same overlap with  $|E_{0,N}\rangle$  by normalization:

$$\langle E_{0,N} | P(t) \rangle = \frac{1}{Z^{1/2}} \sum_{\sigma \in \mathbb{B}_{N,L}} P(\sigma, t) = \frac{1}{Z^{1/2}}, \quad (5)$$

so at asymptotically large times, we have, irrespective of  $P(0)$ ,

$$\langle O(t) \rangle \simeq \frac{1}{Z} \sum_{\sigma} O(\sigma) + c_1 e^{-E_1 t} + \dots, \quad (6)$$

where  $c_1 \propto \langle E_1 | P(0) \rangle$ .

The Hamiltonian  $H$  commutes with the total number of particles  $N$  (or total  $S^z$ ) and the translation operator  $T$  which rotates the particle configuration by a lattice spacing  $T|\sigma_1, \dots, \sigma_L\rangle = |\sigma_2, \dots, \sigma_L, \sigma_1\rangle$ . All eigenstates can then be labelled by  $N, Q$  and the set of configurations with  $N$  particles is  $\mathbb{B}_{N,L} = \{\sigma \in \{0, 1\}^L | \sum_i \sigma_i = N\}$ . The equilibrium distribution and a trivial representation of the translation group (*i.e.*  $T|E_0\rangle = |E_{0,Q=0}\rangle$ ). The ground state, due to the condition  $\sum_{\sigma} H_{\sigma', \sigma} = 0$ , is the uniform superposition of all the particle configurations:

$$|E_{0,N}\rangle = \frac{1}{Z^{1/2}} \sum_{\sigma \in \mathbb{B}_{N,L}} |\sigma\rangle, \quad (7)$$

where  $Z = \binom{L}{N}$ .

This can be used to compute for example the density-density correlation functions using  $O = n_1 n_{x+1}$ . We see that correlation functions will decay exponentially after a time which is the inverse of the lowest energy on which  $P(0)$  has overlap with. For example, if the initial configuration  $P(0)$  is built with using only eigenfunctions with momentum  $Q$ , the decay time will be the inverse of the ground state momentum in the sector  $Q$ ,  $E_{1,N} = E_{0,N,Q}$

$$T_{eq}(Q) = 1/E_{0,N,Q}. \quad (8)$$

We expect  $E_{0,N,Q} \simeq D(\rho)Q^2 + O(Q^4)$  for small  $Q$  and we observe  $D(\rho)$  that decreases monotonically with  $\rho$ . The global ground state  $E_{0,N}$  is in the  $Q = 0$  sector, obviously.

The Hamiltonian is real and positive, the ground state will correspond to zero decay rate. Importantly, the existence of the diffusion cascade[22] restricts straightforward extraction of the diffusion constant in a finite system to the lowest momentum  $Q = 2\pi/L$ , which is what we use henceforth.

### 3. Fermionization and a mean field approximation

In order to proceed with the analysis of the model, we break  $h_{i,j,k}$  into Pauli basis $\ddagger$  and first rewrite the rate matrix as the Hamiltonian of a spin system with  $s^\alpha = \sigma^\alpha/2$  where  $\sigma^\alpha$  are Pauli matrices:

$$\begin{aligned}
 h_{1,2,3} = & \left( s_1^z + \frac{1}{2} \right) \vec{s}_2 \cdot \vec{s}_3 + \left( s_2^z + \frac{1}{2} \right) \vec{s}_3 \cdot \vec{s}_1 + \\
 & + \left( s_3^z + \frac{1}{2} \right) \vec{s}_1 \cdot \vec{s}_2 - \frac{1}{3} \left( s_1^z + s_2^z + s_3^z + \frac{3}{2} \right). \tag{9}
 \end{aligned}$$

This form is also reminiscent of a PXP spin model on a triangular ladder $\S$ . Then we re-write it in terms of hard-core bosons, by defining:  $f = \sigma^-$ ,  $f^\dagger = \sigma^+$ ,  $\sigma^z = 2f^\dagger f - 1$ . After some algebra we have:

$$\begin{aligned}
 h_{1,2,3} = & \frac{1}{2} \left( f_1 f_2 f_2^\dagger f_3^\dagger + f_1^\dagger f_2 f_2^\dagger f_3 + f_1 f_2^\dagger f_3 f_3^\dagger + f_1^\dagger f_2 f_3 f_3^\dagger + f_1 f_1^\dagger f_2 f_3^\dagger \right. \\
 & + \left. f_1 f_1^\dagger f_2^\dagger f_3 \right) - f_2 f_2^\dagger f_3 f_3^\dagger - f_1 f_1^\dagger f_3 f_3^\dagger - f_1 f_1^\dagger f_2 f_2^\dagger + \\
 & + 3f_1 f_1^\dagger f_2 f_2^\dagger f_3 f_3^\dagger. \tag{10}
 \end{aligned}$$

As usual, hard-core bosons  $f_i$  in one dimension can be fermionized via a Jordan-Wigner transformation

$$\begin{aligned}
 \sigma_j^+ = f_j^\dagger &= e^{-i\pi \sum_{k=1}^{j-1} a_k^\dagger a_k} \cdot a_j^\dagger = \prod_{k=1}^{j-1} (1 - 2a_k^\dagger a_k) \cdot a_j^\dagger \\
 \sigma_j^- = f_j &= e^{+i\pi \sum_{k=1}^{j-1} a_k^\dagger a_k} \cdot a_j = \prod_{k=1}^{j-1} (1 - 2a_k^\dagger a_k) \cdot a_j \\
 f_j^\dagger f_j &= a_j^\dagger a_j = \frac{\sigma_j^z + I}{2}
 \end{aligned}$$

to get

$$\begin{aligned}
 h_{1,2,3} = & \frac{1}{2} \left( a_1^\dagger a_2 a_2^\dagger a_3 + a_3^\dagger a_2 a_2^\dagger a_1 + a_1^\dagger a_3 a_3^\dagger a_2 + a_2^\dagger a_3 a_3^\dagger a_1 \right. \\
 & + \left. a_2^\dagger a_1 a_1^\dagger a_3 + a_3^\dagger a_1 a_1^\dagger a_2 \right) \\
 & - a_2 a_2^\dagger a_3 a_3^\dagger - a_1 a_1^\dagger a_3 a_3^\dagger - a_1 a_1^\dagger a_2 a_2^\dagger \\
 & + 3a_1 a_1^\dagger a_2 a_2^\dagger a_3 a_3^\dagger. \tag{11}
 \end{aligned}$$

$\ddagger$  These first technical steps are similar to [24]

$\S$  Recognizing that  $(s_i^z + \frac{1}{2}) \vec{s}_{i+1} \cdot \vec{s}_{i+2} = (s_i^z + \frac{1}{2}) \vec{s}_{i+1} \cdot \vec{s}_{i+2} (s_i^z + \frac{1}{2})$ , and similarly for the other terms. Explicitly,  $H = -\sum_i P_i X_{i+1,i+2,i} P_i + P_{i+1} X_{i+2,i,i+1} P_{i+1} + P_{i+2} X_{i,i+1,i+2} P_{i+2}$ , with  $P_i = (s_i^z + 1/2)$  and  $X_{a,b,c} = \vec{s}_a \cdot \vec{s}_b + P_c$ .

The full Hamiltonian is obtained by summing these terms over all the triangular plaquettes. The resulting fermionic Hamiltonian then can be split into a “conditioned” hopping on the triangle in Fig.2:

$$T = \frac{1}{2} \sum_{\langle i,j,k \rangle} a_i^\dagger (1 - a_j^\dagger a_j) a_k + \text{h.c.}, \quad (12)$$

and a mixed 2-3 fermion density interaction term

$$V = - \sum_{\langle i,j \rangle} (1 - a_i^\dagger a_i) (1 - a_j^\dagger a_j) + 3 \sum_{\langle ijk \rangle} (1 - a_i^\dagger a_i) (1 - a_j^\dagger a_j) (1 - a_k^\dagger a_k), \quad (13)$$

and finally

$$H = T + V. \quad (14)$$

Constrained hopping quantum particles are another interesting subject of recent research in particular for their slow but not many-body localized dynamics, see for example[25]. This Hamiltonian, written in this form, does not seem to be exactly solvable despite being clearly a special case (it is *stoquastic*, i.e. the off-diagonal terms are all of the same sign, and does not have a sign problem either). So, in order to make progress we must make some approximations. Let us see how much mileage we get from a simple mean field approximation. To start, let us consider the ground state. In a given sector  $N$ , the exact ground state is the superposition of all possible configurations of  $N$  particles in  $L$  sites. We have

$$|E_{0,N}\rangle = \frac{1}{Z} \sum_{1 \leq j_1 \leq j_2 \leq \dots \leq j_N \leq L} a_{j_1}^\dagger a_{j_2}^\dagger \dots a_{j_N}^\dagger |0\rangle. \quad (15)$$

If we define the *grand-canonical state* the coherent state

$$|\Psi(z)\rangle = e^{za_1^\dagger} \dots e^{za_L^\dagger} |0\rangle, \quad (16)$$

then it is not difficult to see that

$$|E_{0,N}\rangle = \frac{1}{Z} \oint \frac{dz}{2\pi i} z^{-N-1} |\Psi(z)\rangle. \quad (17)$$

In the large  $N, L$  limit, one can use the saddle point approximation<sup>||</sup> and obtain

$$|E_{0,N}\rangle \simeq \frac{1}{Z^{1/2}} |\Psi(z_s)\rangle, \quad (18)$$

where  $z$  is the *fugacity* at the saddle point (and  $Z = (1 + |z|^2)^L$  is a normalization constant) and it is fixed by the density  $\rho = N/L$ :

$$\langle E_{0,N} | \sum_{x=1, \dots, L} a_x^\dagger a_x | E_{0,N} \rangle = N, \quad (19)$$

<sup>||</sup> This means one can use the saddle point approximation for any observable, which is equivalent to using the approximated vector.

and

$$\langle \Psi(z) | \sum_{x=1, \dots, L} a_x^\dagger a_x | \Psi(z) \rangle = L \frac{|z|^2}{1 + |z|^2} = N. \quad (20)$$

So  $|z|^2 = \rho/(1 - \rho)$  with an arbitrariness of the phase  $\theta = \arg(z)$ .

The grand-canonical state  $|\Psi(z)\rangle$  is then a good state for starting a mean field approximation, with fixed  $\rho = N/L$  (instead of fixed  $N$ , but as usual the fluctuations will not matter) which is good not only at small  $\rho$  but, as it turns out, also in whole range of  $\rho$ .

First of all, consider that the state is factorized so the expectation values of product of operators on different  $x, y$  sites will become the product of expectation values. Therefore it is sufficient to see that

$$\begin{aligned} \langle a_x^\dagger \rangle_{\text{MF}} &= z^*/(1 + |z|^2), \\ \langle a_x \rangle_{\text{MF}} &= z/(1 + |z|^2), \\ \langle a_x^\dagger a_x \rangle_{\text{MF}} &= \rho, \\ \langle a_x^\dagger a_y \rangle_{\text{MF}} &= \rho(1 - \rho) \text{ for } y \neq x. \end{aligned} \quad (21)$$

Inserting these into Eq.(14), we find

$$\langle \Psi(z) | H | \Psi(z) \rangle = \frac{1}{2}(1 - \rho)6\rho(1 - \rho) - 3(1 - \rho)^2 + 3(1 - \rho)^3 = 0. \quad (22)$$

As we know that the exact GS energy is  $E_{N,0} = 0$  in any sector  $N$  we now understand what it means.  $\Psi(z)$  is a weighted superposition of all the GS's in all the sectors. By relaxing the particle number conservation we can proceed with the calculation of the spectrum of the quasiparticle of the model.

The MF treatment of excitations on top of the ground state can be obtained in the Hartee-Fock approximation (see for example [28], Chapter 5) by substituting the  $a_x^\dagger a_x$  terms with their expectation value on the MF GS, we therefore obtain the effective Hartree-Fock Hamiltonian

$$H_{\text{HF}} = \sum_{\langle i,j,k \rangle} \frac{1}{2}(1 - \rho) \left( a_i^\dagger a_j + a_j^\dagger a_i + a_i^\dagger a_k + a_k^\dagger a_i + a_j^\dagger a_k + a_k^\dagger a_j \right) - 3(1 - \rho)^2 + 3(1 - \rho)^3. \quad (23)$$

The last term is the interaction energy estimated in MF, a constant which we can ignore, while the first term is the hopping on a triangular ladder, which has dispersion law:

$$\epsilon_k = (3 - \cos(2k) - 2 \cos(k))(1 - \rho) \simeq 3(1 - \rho)k^2. \quad (24)$$

The quasi-particles therefore have an effective mass  $m = \frac{1}{6}(1 - \rho)^{-1}$  which diverges as  $\rho \rightarrow 1$ . The quasiparticles are created by acting with  $a_k^\dagger$  on the coherent state  $|\Psi(z)\rangle$  and they have energy  $\epsilon_k = \langle \Psi(z) | a_k H a_k^\dagger | \Psi(z) \rangle$ . The HF Hamiltonian for the quasiparticle excitations is

$$H_{\text{HF}} = \sum_k \epsilon_k a_k^\dagger a_k - 3(1 - \rho)^2 + 3(1 - \rho)^3. \quad (25)$$

Therefore  $[a_k^\dagger, H] = \epsilon_k a_k^\dagger$  which shows that  $\epsilon_k$  determine the decay rate of the state  $a_k^\dagger |\Psi(z)\rangle$ .

We can now go back to the random dynamics of the classical particles by extracting the diffusion coefficient from the lowest energy  $\epsilon_Q$ , to the first excited state which is in the  $Q = 2\pi/L \ll 1$  sector as  $\epsilon_Q = D_1 Q^2 + \dots$ . The MF prediction for the diffusion coefficient is then:

$$D_{\text{MF}} = 3(1 - \rho). \tag{26}$$

This simple form explains very well the numerical data, up to large density  $\rho \sim 5/6$ . However, for  $\rho > 1/2$  and in particular  $\rho \gtrsim 2/3$  the system size dependence becomes important, and this is due to the number of accessible configurations decreasing considerably. In fact, we will see that an exponential number of configurations becomes immobile or *jammed* and this influences the dynamics considerably.

#### 4. Large densities and the appearance of jammed configurations

As we increase the density past the critical value  $\rho = 2/3$  a series of particle configurations appear which are stuck or jammed, namely that cannot be moved by our dynamical rules. They are trivial ground states of the Hamiltonian since  $H|\sigma\rangle = 0$  for each of these. At exactly  $\rho = 2/3$  one can see that the single configuration  $\sigma = 110110110\dots$  and its 2 translates by  $T$  are jammed. At this point 3 more ground states appear in the spectrum. ¶

As  $\rho > 2/3$  the number of such configurations becomes exponential in  $L$ , and therefore we define an entropy of jammed configurations  $s_j = (\ln \mathcal{N})/L$ . Computing the entropy of such configurations  $\mathcal{N}$  using the tools of statistical mechanics is not difficult: Fixing the first vertex to be empty (therefore quotienting wrt to translations which introduces at most a factor  $L$  which does not change the entropy), we have sequence of  $n_1 \geq 2$  ones, then an isolated 0, then a sequence of  $n_2 \geq 2$  ones, then another zero and so on. So the number of sequences of 1 is equal to the number of zeros  $N_0 = L - N$ .

So we can compute the number of sequences of  $N_0 = L - N$  numbers  $n_i \geq 2$  that sum to  $N$ . So defining the set of integer sequences  $\mathbb{S} = \{\{n_i\}_{i=1}^{N_0} | n_i \geq 2\}$

$$\mathcal{N}(N) = \sum_{\{n_i\} \in \mathbb{S}} \delta_{\sum_{i=1}^{N_0} n_i, N}. \tag{27}$$

We need to compute this number for large  $N, L$  fixing  $\rho = N/L$ . To do this we first

¶ Notice that the total number of such configurations of length  $L$ , *not constrained* to have a given density  $\rho$ , is a known combinatorial problem which has as solution the sequence A000930 of OEIS, also known as Narayana's cows sequence: 1, 2, 3, 4, 6, 9, 13, 19, 28, 41, 60, 88, ... . This number grows asymptotically like  $x^L$  where  $x = 1.4655\dots$  is the only real solution of the equation  $x^3 - x^2 + 1 = 0$ . Notice also that this is exactly the exponential of the maximum of the entropy Eq.(33),  $x = \exp(s_j(\rho^*))$  which is achieved at  $\rho^* = 0.80574$ . So the typical frozen configurations have density  $\rho = \rho^*$  and there are  $x^L$  of them.



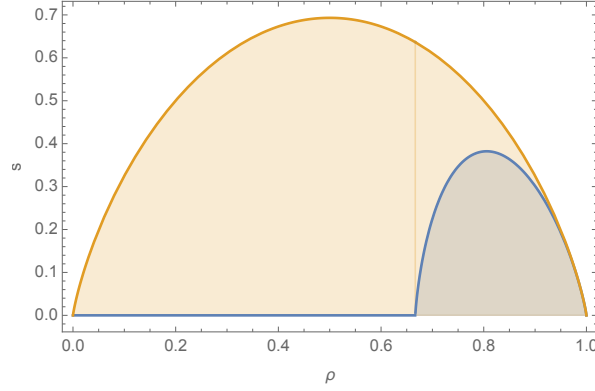


**Figure 3.** Entropy of jammed configurations (blue) and total entropy of the system (yellow).

compute the generating function (grand-canonical ensemble)

$$\mathcal{N}(z) = \sum_{N=0}^{\infty} \mathcal{N}(N) z^N, \quad (28)$$

which we will eventually invert using:

$$\mathcal{N}(N) = \oint \frac{dz}{2\pi i} z^{-N-1} \mathcal{N}(z). \quad (29)$$

Now,  $\mathcal{N}(z)$  is an unconstrained geometric series:

$$\mathcal{N}(z) = \sum_{n_1 \geq 2, \dots, n_{N_0} \geq 2} z^{\sum_{i=1}^{N_0} n_i} = \frac{z^{2N_0}}{(1-z)^{N_0}}. \quad (30)$$

So

$$\mathcal{N}(N) = \oint \frac{dz}{2\pi i} z^{-N-1} \frac{z^{2N_0}}{(1-z)^{N_0}} \quad (31)$$

and we can evaluate this integral for large  $N_0 = (1-\rho)L$  using the saddle point method. After some straightforward calculations one gets

$$\mathcal{N}(N) \simeq e^{Ls(\rho)} \quad (32)$$

with

$$s_j(\rho) = (\rho - 1) \log \left( \frac{1-\rho}{2\rho-1} \right) + (2-3\rho) \log \left( \frac{3\rho-2}{2\rho-1} \right). \quad (33)$$

This curve is depicted in Fig.3, together with the total entropy  $s(\rho) = -\rho \ln \rho - (1-\rho) \ln(1-\rho)$ . It reaches a maximum at a value  $\rho^* = 0.80574\dots$ . As the density is increased, one can see that a larger fraction of the configurations become jammed, as the difference between the total entropy and the entropy of the jammed configurations goes to zero (see Figure 3) as  $s(\rho) - s_j(\rho) \simeq 2(\rho-1)^2 + \dots$

If the initial probability distribution  $P(0)$  has overlap with one of these, then it will *never* reach the equipartite equilibrium  $P_{eq} = \frac{1}{Z} \sum_{\sigma} |\sigma\rangle = \frac{1}{Z^{1/2}} |E_0\rangle$ . However, if the

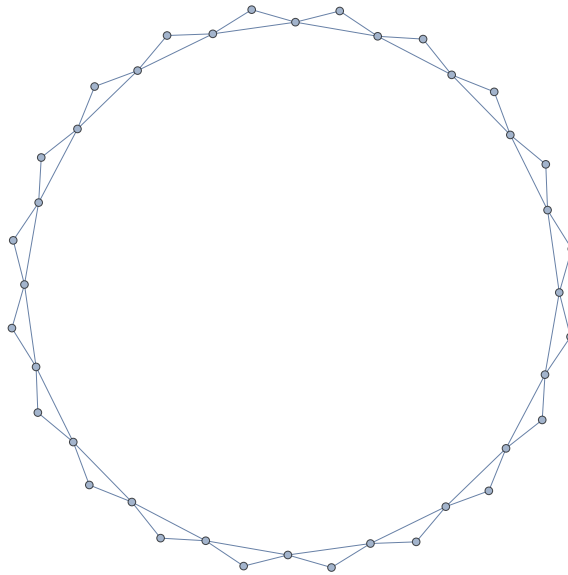


**Figure 4.** Reduced Hamiltonian of the  $L = 20, N = 18$  configuration. It contains  $2L = 40$  unjammed configurations, which are connected either to 2 or 4 other configurations. Amplitudes are  $-1/2$  over all the off-diagonal matrix elements.

initial configuration *does not* have overlap with any jammed configuration, it will decay to the equilibrium state in a time which is again dictated by diffusion  $T_{eq} = L^2/D$ . The value of  $D$  must be extracted from numerics. It turns out, again, to be well described by the MF result  $D = 3(1 - \rho)$ , see Fig.1, although with relevant finite-size corrections.

## 5. Close to maximum density: holes and doublons

Near  $\rho = 1$  we can still find a diffusion coefficient. We consider the sectors  $N = L, L - 1, L - 2, \dots$ . The sector  $N = L$  has only one state, the completely full one: this state is clearly jammed. The sector  $N = L - 1$  has  $N$  states (the positions of the single hole) but they are all jammed as well since one needs two holes at least for them to be mobile.

The sector  $N = L - 2$  shows the first unjammed configurations, although the holes have to move together to be mobile, separated by at most one particle. So we have  $2L$  unjammed configurations. We call these configurations a *doublon*. The configuration with two holes separated by a particle  $\dots 1101011\dots$  can move in two possible ways:  $\dots 1110011\dots$ ,  $\dots 1100111\dots$ , while the configuration with two neighboring holes  $\dots 110011\dots$  can move in 4 possible ways. All amplitudes are  $-1/2$  and the diagonal terms are 1 and 2 respectively (to ensure  $\sum_i H_{ij} = 0$ ). The graph of possible motions is as in Figure 4.

The effective Hamiltonian of the doublon is now a chain decorated with triangles.

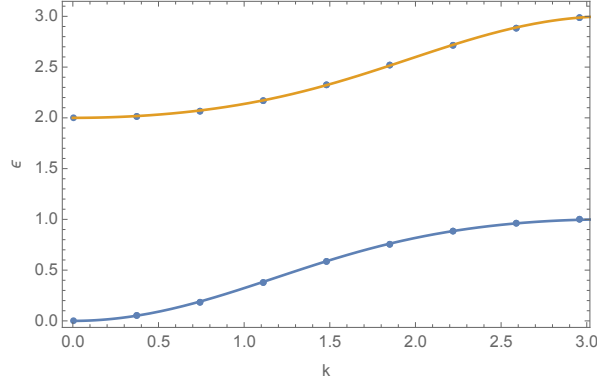


**Figure 5.** Energy vs momentum of the doublons eigenstates, in the case  $N = 15, L = 17$ . Numerics (dots), and analytics (lines) in Eq.(37).

Numbering the vertices  $i = 1, \dots, 2L$ , the equations for the doublon amplitudes  $\psi_i$  are

$$E\psi_{i+2} = 2\psi_{i+2} - \frac{1}{2}\psi_{i+1} - \frac{1}{2}\psi_i - \frac{1}{2}\psi_{i+3} - \frac{1}{2}\psi_{i+4} \quad (34)$$

$$E\psi_{i+1} = \psi_{i+1} - \frac{1}{2}\psi_i - \frac{1}{2}\psi_{i+2}. \quad (35)$$

Separating the odd (connected to 2) and even (connected to 4) configurations, and using the plane wave ansatz  $\psi_{j,o} = a_1 e^{ijk}$ ,  $\psi_{j,e} = a_2 e^{ijk}$  respectively, with now  $j = 1, \dots, L$  we find the eigenvalues by diagonalizing the reduced matrix

$$M = \begin{pmatrix} 1 & -\frac{1}{2} - \frac{e^{ik}}{2} \\ -\frac{1}{2} - \frac{e^{-ik}}{2} & 2 - \cos(k) \end{pmatrix}. \quad (36)$$

The eigenvalues form a sound and an optical branch (in the first the particles move together, in the second they oscillate around a common center of mass):

$$\epsilon_k = \frac{1}{4} \left( -2 \cos(k) \pm \sqrt{2} \sqrt{\cos(2k) + 7 + 6} \right). \quad (37)$$

At small  $k$  we have

$$\epsilon_{k,1} = \frac{3}{8}k^2 + O(k^4), \quad (38)$$

$$\epsilon_{k,2} = 2 + \frac{1}{8}k^2 + O(k^4). \quad (39)$$

Remembering that the minimum  $k = Q = 2\pi/L$  we find that the diffusion coefficient of 2 holes is

$$D_{N=L-2,L} \equiv \epsilon_{k,1} \frac{L^2}{(2\pi)^2} \rightarrow \frac{3}{8}. \quad (40)$$

So the diffusion coefficient is small but not zero for  $N = L - 2$ . This compares perfectly with the numerics (blue points in Fig.8).

The next sector is  $N = L - 3$  which contains 3 holes. Again, the only mobile configurations have at least two holes close to each other (distance 1 or 2 like in the previous case) forming a doublon and a single hole anywhere in the remaining  $L - 3$

sites of the chain. If the third hole is at distance  $\geq 2$  from the doublon it cannot move and is stuck there. So, to reach the equilibrium configuration in which the hole is at, say  $x$ , and the doublon is at  $y$ , the three holes must move together and the doublon must deposit the hole there. Therefore the equilibrium time is proportional to the time necessary for a doublon to pick up and deposit a hole in one of the  $L - 3$  possible states. This time is

$$T_{N=L-3}^{eq} \sim (L - 3) \times T_{N=L-2}^{eq} \sim L \times L^2, \quad (41)$$

which formally correspond to a diffusion coefficient

$$D_{N=L-3} \sim 1/L, \quad (42)$$

and in practice corresponds to subdiffusion.

For larger  $n \geq 3$ , a certain number of doublons is in the spectrum of the theory so one would expect the equilibrium process to be dominated by these and therefore the timescale to be again

$$T_{N=L-n}^{eq} \sim L \times L^2. \quad (43)$$

This suggests that, insisting on the definition of a diffusion coefficient, this is  $D_{N=L-n} = c_n L^{-1}$ . The numerics shows that  $c_3 = 3/8$  and  $c_4 = 3/4$  which makes us conjecture  $c_n = (3/8)[n/2]$  simply proportional to the number of doublons in the sector. Once the density of doublons becomes finite, so  $(1 - \rho) = O(1)$ , one expects a finite diffusion coefficient  $D$ . Whether we can confidently say that this equals the MF predictions  $D = 3(1 - \rho)$ , it is discussed in the next Section.

## 6. Exact numerical results

The classical model can be simulated by a random process in which one picks a random triangular plaquette and then, if it qualifies, i.e. it contains a single particle, makes a random move of the particle on one of the other two, empty, vertices (if it does not qualify, then nothing happens). Such a random process, quick to implement, leads to correlation functions decay among observables. The decays are eventually exponential,<sup>+</sup> the longest time-scale being the equilibrium time  $T_{eq}$  discussed above.

Alternatively, one can write a (sparse) rate matrix, and find the gap above the ground state with Lanczos-like algorithms. In this way we can access mesoscopic ( $L = 30$ ) to large ( $L = 200$ ) system sizes, depending on the number of particles. We have preferred this latter method, by which we have produced the figures in this section.

### 6.1. Low density limit

In the low-density limit we expect the prediction of the fermionic MF theory to be correct.  $D = 3(1 - \rho)$ , in particular  $D = 3$  for  $\rho = 0$ , which is reproduced by  $O(1)$

<sup>+</sup> As already mentioned in Sec. 2 the existence of the diffusion cascade obstructs naive  $D(\rho)Q^2$  dispersion of the decay rate. Briefly, while initial temporal decay may follow  $D(\rho)Q^2$  the late time decay rate is much slower,  $\sim Q^2/n$ , where  $n = LQ/2\pi \geq 1$ . This is the focus of a companion paper[22]

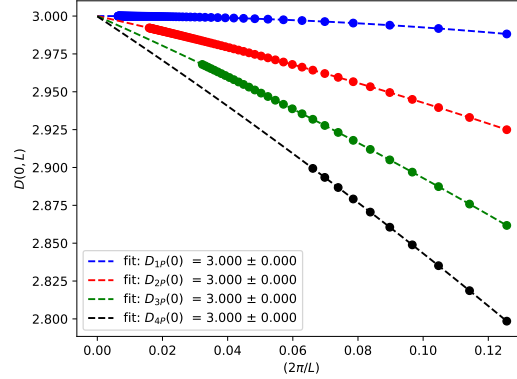


**Figure 6.** Diffusion coefficient vs  $Q = \frac{2\pi}{L}$  for  $\rho \rightarrow 0$  with quadratic fit.  $L = 50, 60, \dots, 990$  for 1 particle (blue).  $L = 50, 55, \dots, 395$  for 2 particles (red).  $L = 50, 55, \dots, 195$  for 3 particles (green). And  $L = 50, 55, \dots, 95$  for 4 particles (black). They all extrapolate to the theoretical value  $D = 3$  valid for density  $\rho = 0$ .

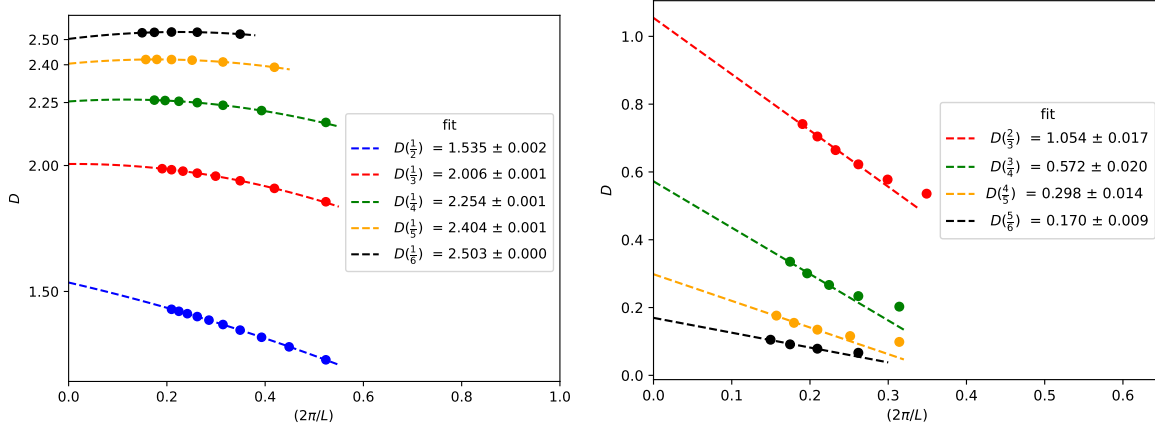


**Figure 7.** (Left) Diffusion coefficient vs  $Q = \frac{2\pi}{L}$  with a quadratic fit and the values predicted by MFT  $D = 3(1 - \rho)$ .  $L = 8, 10, \dots, 30$  for  $\rho = 1/2$  (blue).  $L = 9, 12, \dots, 33$  for  $\rho = 1/3$  (red).  $L = 12, 16, \dots, 36$  for  $\rho = 1/4$  (green).  $L = 15, 20, \dots, 40$  for  $\rho = 1/5$  (orange). And  $L = 18, 24, \dots, 42$  for  $\rho = 1/6$  (black). (Right) Diffusion coefficient vs  $Q = \frac{2\pi}{L}$  with linear fit.  $L = 18, 21, \dots, 33$  for  $\rho = 2/3$  (red).  $L = 20, 24, \dots, 36$  for  $\rho = 3/4$  (green).  $L = 20, 25, \dots, 40$  for  $\rho = 4/5$  (orange). And  $L = 24, 30, \dots, 42$  for  $\rho = 5/6$  (black).

particles as  $L \rightarrow \infty$  as can be seen in 6. Notice the different number of particles give rise to different  $1/L$  corrections but not the final result.

Going to larger densities the result does not change substantially, and the prediction  $D = 3(1 - \rho)$  is satisfied up to  $\rho = 1/2$  as seen in Figure 7, although again, larger densities correspond to large finite-size corrections.

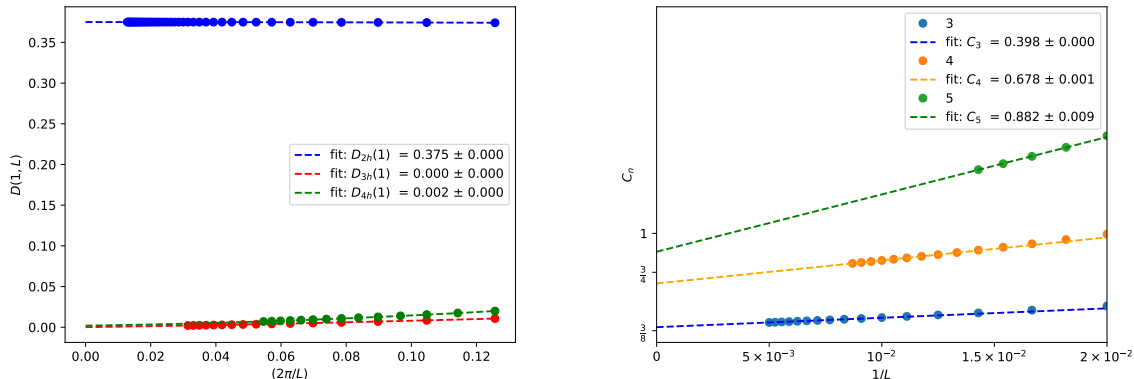


**Figure 8.** (Left) Diffusion coefficient vs  $Q = \frac{2\pi}{L}$  for  $\rho \rightarrow 1$  with quadratic fit.  $L = 50, 60, \dots, 490$  for 2 holes (blue).  $L = 50, 60, \dots, 200$  for 3 holes (red).  $L = 50, 55, \dots, 115$  for 4 holes (green). (Right) For  $n \geq 3$  holes the coefficient  $c_n$  defined as  $c_n = LD_{N-n, L}$  vs  $1/L$  and the extrapolated value.

## 6.2. After jamming and towards isolated doublons

Crossing the transition at  $\rho = 2/3$ , where one starts to have jammed configurations, the finite-size corrections become important. This might be due to the fact that the number of accessible configurations from an initial, unjammed one, can be considerably smaller than expected, which typically increases the finite-size correction. A simple linear extrapolation in  $1/L$  does agree with the prediction of MF theory within an acceptable 5% margin. See figs. 7. However, the limit  $N = L - n$  with  $L \rightarrow \infty, n = O(1)$  falls back into the analysis of the previous section. The diffusion coefficient for  $n = 2$  is  $D = 3/8$  while for  $n \geq 3$  is  $D_n = c_n/L$  with  $c_3 = 3/8, c_4 = 3/4$  and we conjecture  $c_n = (3/8)[n/2]$  where  $[n/2]$  is the integer part of  $n/2$ , which counts the number of doublons. However, already for  $n = 5$  the finite-size corrections are so large that we cannot confirm this prediction (see Fig.8, right panel).

## 7. Conclusions and further work

We have designed and solved, in the mean-field approximation, a kinetically constrained model of particles hopping on a triangular ladder. The solution is obtained by a classical-quantum mapping to a model of interacting fermions. The diffusion coefficient is the inverse of the mass of the quasiparticles, which can be computed in the mean-field approximation and returns a monotonically decreasing diffusion coefficient in striking agreement with the numerics in a large interval of densities. Two sets of numerics have confirmed these results: both Montecarlo calculations on the classical particle model and exact diagonalization of the quantum Hamiltonian. As directions for further work, one should try to either go beyond the mean-field approximation or, since we see little deviations from the MF result in the numerics, prove its exactness. Moreover,

the model can be easily generalized to a triangular lattice in 2 dimensions \* where one still finds jammed configurations and the quantum model is a model of hard-core bosons with conditioned hopping. We also notice that a classical-quantum mapping on a fermionic model, like the one devised in this paper, might be useful to get a field-theory approach to other KCPs or facilitated spin models, which is fundamentally different from other known ones, which are based on mode-coupling theory (see [21, 20] and references therein) or other mappings to many-body models, followed by a different kind of approximation [24].

## 8. Acknowledgements

A.S. would like to thank the Graduate Center of CUNY for hospitality during a visit in July 2024, when this project got started. The work of A.S. was funded by the European Union - NextGenerationEU under the project NRRP “National Centre for HPC, Big Data and Quantum Computing (HPC)” CN00000013 (CUP D43C22001240001) [MUR Decree n. 341- 15/03/2022] - Cascade Call launched by SPOKE 10 POLIMI: “CQEB” project. A.R. and V.O. would like to thank Sarang Gopalakrishnan and Paolo Glorioso for collaboration on a related work[22].

.....

## 9. Bibliography

- [1] Dmitry A Abanin, Ehud Altman, Immanuel Bloch, and Maksym Serbyn. Colloquium: Many-body localization, thermalization, and entanglement. *Reviews of Modern Physics*, 91(2):021001, 2019.
- [2] Denis M Basko, Igor L Aleiner, and Boris L Altshuler. Metal–insulator transition in a weakly interacting many-electron system with localized single-particle states. *Annals of physics*, 321(5):1126–1205, 2006.
- [3] Robert P Behringer and Bulbul Chakraborty. The physics of jamming for granular materials: a review. *Reports on Progress in Physics*, 82(1):012601, 2018.
- [4] Lorenzo Bertini, Alberto De Sole, Davide Gabrielli, Giovanni Jona-Lasinio, and C233569507120473 Landim. Stochastic interacting particle systems out of equilibrium. *Journal of Statistical Mechanics: Theory and Experiment*, 2007(07):P07014, 2007.
- [5] Luca D’Alessio, Yariv Kafri, Anatoli Polkovnikov, and Marcos Rigol. From quantum chaos and eigenstate thermalization to statistical mechanics and thermodynamics. *Advances in Physics*, 65(3):239–362, 2016.
- [6] B. Derrida. An exactly soluble non-equilibrium system: The asymmetric simple exclusion process. *Physics Reports*, 301(1):65–83, 1998.
- [7] Joshua M Deutsch. Eigenstate thermalization hypothesis. *Reports on Progress in Physics*, 81(8):082001, 2018.
- [8] Aleksandar Donev, Salvatore Torquato, Frank H Stillinger, and Robert Connelly. Jamming in hard sphere and disk packings. *Journal of applied physics*, 95(3):989–999, 2004.
- [9] Samuel Frederick Edwards and Phil W Anderson. Theory of spin glasses. *Journal of Physics F: Metal Physics*, 5(5):965, 1975.

\* We thank Frank Pollman for this suggestion, which opens the way to an unexpected generalization of our work.

- [10] Zhaoyu Han and Steven A Kivelson. Models of interacting bosons with exact ground states: a unified approach. *arXiv preprint arXiv:2408.15319*, 2024.
- [11] Scott Kirkpatrick and Bart Selman. Critical behavior in the satisfiability of random boolean expressions. *Science*, 264(5163):1297–1301, 1994.
- [12] Marc Mézard and Giorgio Parisi. Glasses and replicas. *Structural Glasses and Supercooled Liquids: Theory, Experiment, and Applications*, pages 151–191, 2012.
- [13] Marc Mézard, Giorgio Parisi, and Miguel Angel Virasoro. *Spin glass theory and beyond: An Introduction to the Replica Method and Its Applications*, volume 9. World Scientific Publishing Company, 1987.
- [14] Marc Mézard, Giorgio Parisi, and Riccardo Zecchina. Analytic and algorithmic solution of random satisfiability problems. *Science*, 297(5582):812–815, 2002.
- [15] Marc Mézard and Riccardo Zecchina. Random k-satisfiability problem: From an analytic solution to an efficient algorithm. *Physical Review E*, 66(5):056126, 2002.
- [16] Rahul Nandkishore and David A Huse. Many-body localization and thermalization in quantum statistical mechanics. *Annu. Rev. Condens. Matter Phys.*, 6(1):15–38, 2015.
- [17] Vadim Oganesyan and David A Huse. Localization of interacting fermions at high temperature. *Physical Review B—Condensed Matter and Materials Physics*, 75(15):155111, 2007.
- [18] Giorgio Parisi. Nobel lecture: Multiple equilibria. *Reviews of Modern Physics*, 95(3):030501, 2023.
- [19] Giorgio Parisi and Francesco Zamponi. Mean-field theory of hard sphere glasses and jamming. *Reviews of Modern Physics*, 82(1):789–845, 2010.
- [20] Gianmarco Perrupato and Tommaso Rizzo. Exact dynamical equations for kinetically-constrained-models. *arXiv preprint arXiv:2212.05132*, 2022.
- [21] Steven J Pitts, Thomas Young, and Hans C Andersen. Facilitated spin models, mode coupling theory, and ergodic–nonergodic transitions. *The Journal of Chemical Physics*, 113(19):8671–8679, 2000.
- [22] Abhishek Raj, Paolo Glorioso, Sarang Gopalakrishnan, and Vadim Oganesyan. Diffusion cascade in a model of interacting random walkers. *arXiv preprint arXiv:2412.05222*, 2024.
- [23] F. Ritort and P. Sollich. Glassy dynamics of kinetically constrained models. *Advances in Physics*, 52(4):219–342, 2003.
- [24] Michael Schulz and Steffen Trimper. An analytical approach to the fredrickson–andersen model in one dimension. *International Journal of Modern Physics B*, 11(24):2927–2940, 1997.
- [25] Piotr Sierant, Eduardo Gonzalez Lazo, Marcello Dalmonte, Antonello Scardicchio, and Jakub Zakrzewski. Constraint-induced delocalization. *Physical Review Letters*, 127(12):126603, 2021.
- [26] Piotr Sierant, Maciej Lewenstein, Antonello Scardicchio, Lev Vidmar, and Jakub Zakrzewski. Many-body localization in the age of classical computing. *arXiv preprint arXiv:2403.07111*, 2024.
- [27] Mark Srednicki. Chaos and quantum thermalization. *Physical review e*, 50(2):888, 1994.
- [28] Xiao-Gang Wen. *Quantum field theory of many-body systems: From the origin of sound to an origin of light and electrons*. Oxford university press, 2004.